Chapter 9
Optical Motion Magnification for Vibration-based Condition Monitoring of Hydroelectric Turbines

Hussein Ali Ahmad, Marco Civera, Cecilia Surace, Christopher Niezrecki, and Alessandro Sabato

Abstract Hydropower plants are often viewed as environmentally sustainable and economically efficient sources of energy, characterized by low operating costs and the ability to support grid stability through reservoir storage. However, the long-term reliability and performance of these facilities heavily depend on effective monitoring of critical components, particularly hydroelectric turbines. Traditional condition monitoring methods often rely on contact or line-of-sight sensors, which can be intrusive, costly, or difficult to install in certain environments. This study investigates the use of Optical Motion Magnification (OMM) as a novel approach for monitoring the dynamic behavior of turbine components. OMM works by amplifying subtle motions in high-resolution video footage, allowing visualization of fine-scale vibrations that are otherwise imperceptible to the human eye. This method enables the detection of early signs of mechanical degradation without physically interacting with the equipment. A series of laboratory-based experiments were conducted to evaluate the effectiveness of OMM in comparison to conventional non-contact sensors, including proximity probes and laser displacement systems. Key performance metrics such as sensitivity, accuracy, and fault detection capability were analyzed. The results indicate that OMM successfully captures the essential features of vibrational behavior, making it a promising alternative for condition monitoring in hydropower settings. Due to its adaptability, non-invasiveness, and potential for lower implementation costs, OMM offers a compelling option for augmenting or replacing traditional sensing technologies.

Keywords Optical Motion Magnification · Condition Monitoring · Computer Vision · Hydroelectric Turbines · Non-contact Sensors

Introduction

Condition monitoring (CM) plays a critical role in ensuring the reliability, efficiency, and longevity of rotating machinery across various industries, including power generation [1], manufacturing [2], and transportation [3]. In the context of hydropower facilities, turbine systems are particularly vital, as they operate under high loads and harsh environmental conditions for extended periods [4]. Failures in hydropower turbine components can lead to costly downtime, reduced efficiency, and even catastrophic damage, making predictive maintenance and early fault detection essential [5]. To address this, CM systems are commonly employed to detect abnormalities in machine behavior before they escalate into major failures.

Traditional CM approaches often rely on contact-based sensors such as accelerometers, proximity probes, and laser displacement sensors to extract global changes in the dynamic properties of the inspected asset [6, 7]. While effective in many applications, these technologies come with notable limitations. Their installation can be invasive, requiring physical access to critical components that may be difficult to reach or housed in sealed enclosures. Additionally, these sensors can be expensive, prone to wear, and require regular maintenance. In hydropower plants, where space constraints, fluid exposure,

Hussein Ali Ahmad · Marco Civera(✉) · Cecilia Surace
Department of Structural, Geotechnical and Building Engineering, Politecnico di Torino, 10129 Turin, Italy
e-mail: s313580@studenti.polito.it; marco.civera@polito.it; cecilia.surace@polito.it

Christopher Niezrecki · Alessandro Sabato
Department of Mechanical and Industrial Engineering, University of Massachusetts Lowell, Lowell, MA 01854, United States
e-mail: Christopher_Niezrecki@uml.edu; alessandro_sabato@uml.edu

© The Author(s), under exclusive license to River Publishers 2026

Kristin B. Zimmerman, PhD (eds.), *Computer Vision and SLDV for Structural Dynamics, 2026, Vol. 6*, Conference Proceedings of the Society for Experimental Mechanics Series, https://doi.org/10.13052/rp-9788743814177

and operational complexity pose significant challenges, these limitations can compromise the feasibility and effectiveness of conventional sensing solutions.

To overcome these barriers, this study explores the use of Optical Motion Magnification (OMM) as a non-contact, vision-based alternative for monitoring the dynamic behavior of hydropower turbine components. OMM amplifies small motions in high-resolution video recordings, making otherwise imperceptible vibrations visible and measurable [8, 9]. This technique offers the potential to detect early-stage mechanical faults in a non-invasive and cost-effective manner, without disrupting equipment operation.

The objective of this study is to evaluate the feasibility and performance of OMM for condition monitoring in hydropower applications. Through a series of controlled experiments, the dynamic response of turbine components is analyzed using OMM and compared against conventional sensor outputs. The findings aim to determine whether OMM can serve as a viable supplement, or even an alternative, to traditional monitoring methods, particularly in environments where sensor placement is burdensome or intrusive. This paper is organized as follows. Section 2 (Related studies) summarizes the most used techniques for CM of rotating machinery and some of the applications of OMM. Section 3 (Laboratory experiments) describes the tests performed to validate the accuracy of OMM in measuring the vibration of rotating machinery in a controlled environment. Section 4 (Field tests) provides an overview of the results obtained when OMM is used to measure the displacement of an operational hydropower turbine. Finally, Section 5 (Conclusions) summarizes the main findings of this study and provides insight into future directions.

Related Studies and Research Context

Overview of condition monitoring techniques for rotating machinery

Rotating machinery, such as motors, pumps, compressors, turbines, and gearboxes, is integral to many industrial applications, particularly in hydropower plants, where unexpected breakdowns can result in significant production losses, safety hazards, and increased maintenance costs. Over the decades, various techniques have been developed to monitor the health of such equipment. Vibration analysis remains one of the most established and widely used CM techniques for rotating machinery [10, 11]. It relies on sensors such as accelerometers or velocity transducers mounted on key components (e.g., bearings, casings) to detect abnormal vibration signatures. The underlying principle is that mechanical defects, such as imbalance, misalignment, bearing faults, or gear damage, induce characteristic changes in vibration frequency and amplitude. Signal processing techniques are used to analyze these vibrations and identify patterns or changes in those patterns that are representative of the onset of damage [12]. Vibration analysis offers high sensitivity and diagnostic capability, but it requires careful sensor placement, experience in interpreting spectral patterns, and often necessitates shutdown for accurate assessments in some instances.

Ultrasound CM is another popular approach that uses high-frequency acoustic waves to detect anomalies, particularly crack formation in bearings [13]. Ultrasonic detectors can sense friction, turbulence, and impact-generated waves in the 20 kHz–100 kHz range. These signals often precede the onset of detectable vibration or thermal anomalies, making ultrasound highly effective for early detection of bearing lubrication issues, arcing in electrical components, and valve leakages [14]. The technique is particularly effective in high-noise environments and offers both airborne and contact modes. However, interpreting ultrasonic signals can be less intuitive and typically requires skilled personnel. Similarly to ultrasound, to ultrasound, acoustic emission (AE) monitoring involves capturing high-frequency elastic waves generated by the rapid release of energy from localized sources within materials. In rotating machinery, AE can detect crack initiation, corrosion, and material deformation [15]. AE sensors are extremely sensitive and capable of identifying microscopic defects that are often undetectable by other methods. AE techniques are particularly useful for real-time monitoring of critical components under load. However, they are susceptible to ambient noise and require signal filtering and pattern recognition techniques for reliable fault classification.

To conclude, Infrared thermography (IRT) detects temperature anomalies on the surface of machinery by capturing emitted infrared radiation. Faults such as misalignment, imbalance, and frictional heating often manifest as localized hotspots, which can be visually identified in thermal images [16]. IRT is non-contact, fast, and suitable for live monitoring without disrupting operations. It is especially effective for electrical systems, lubrication faults, and misaligned couplings [17], while its applications in the hydropower domain are quite limited. Additionally, its effectiveness is limited in identifying faults that do not result in significant thermal changes, and environmental factors (e.g., airflow, emissivity variations) can impact accuracy. For a detailed overview of CM techniques for hydropower turbines, interested readers can refer to [18, 19]. These traditional techniques, while effective, often require complex setups, high expertise, and in some cases, contact-based sensing, which may not always be feasible. This has led to increased interest in non-contact, image-based techniques such as optical motion magnification [20, 21].

Principles and Applications of Optical Motion Magnification

Optical motion magnification (OMM) is a computer vision technique that visually enhances subtle motions in video recordings, making them perceptible to the human eye or measurable through image processing. Unlike traditional methods, OMM enables full-field visualization of structural or mechanical vibrations without physical sensors, allowing safe, remote diagnostics and intuitive fault detection [22].

OMM techniques can be broadly categorized into two methodological frameworks: Eulerian and Lagrangian [23]. The Eulerian approach analyzes intensity changes at fixed spatial locations over time. Each pixel in a video is considered a temporal signal, and motion is inferred from periodic changes in intensity caused by subtle displacements. A temporal band-pass filter is applied to isolate specific frequency bands corresponding to mechanical vibrations. The resulting filtered signals are amplified and recombined with the original video, producing a visually enhanced version of motion. Eulerian techniques are computationally efficient and particularly effective for small, linear displacements. In contrast, the Lagrangian approach tracks the displacement of features or pixels over time. Optical flow or block matching algorithms are used to estimate the trajectory of points, and the motion vectors are amplified before rendering the output. This method is well-suited for larger or non-linear deformations but is generally more computationally intensive and sensitive to tracking errors or noise.

The general OMM workflow begins with the acquisition of a high-frame-rate video of the target machinery. The video is decomposed either spatially (e.g., using Laplacian pyramids or wavelets) and temporally to extract motion information. The filtered signals are then amplified by a magnification factor α, which depends on noise sensitivity and the desired visibility [9]. The amplified signals are added back to the original video frames to create an output that visually exaggerates the motion while preserving the spatial structure. Key parameters such as magnification factor, temporal bandwidth, and filter type must be carefully chosen to prevent artifacts, maintain fidelity, and avoid ghosting [24]. Examples of applications of OMM include operational modal analysis [25–29], monitoring of structures with cracks [30], vibrating panels [31], as well as wind turbine foundations [32, 33]. An evaluation of the performance of this method for CM of hydropower turbines is missing and motivates this study.

Laboratory Experiments

To assess the precision and feasibility of video-based vibration measurement for CM of rotating machinery, a series of laboratory experiments were conducted. The objective was to evaluate the OMM accuracy in capturing the vertical displacements of an axle test rig with varying off-axis mass configurations, and to compare its performance with that of conventional sensing methods. In the experiments, the test rig, shown in Figure 1a, was deliberately unbalanced by attaching masses to the rotating shaft. The resulting dynamic response was simultaneously measured using a high-speed camera and a laser displacement sensor. Masses ranging from 0 to 8×10^{-3} kg were incrementally added in steps of 2×10^{-3} kg, and the rig was operated at a constant rotational speed of 2,400 rpm. Video recordings were captured using a 5-megapixel IRIS MS camera equipped with a 25mm lens, positioned approximately 0.5 meters from the setup, and acquiring images at 1,400 frames per second (fps). The collected videos were processed using the software Motion Amplification, developed by RDI Technologies, to extract both the vertical displacement of the shaft and the system's frequency domain response under each test condition. Concurrently, a Keyence LK-G402 laser displacement sensor was employed to acquire ground-truth vertical displacement data at a sampling rate of 1,000 Hz. An overview of the experimental setup is provided in Figure 1b. To ensure statistical robustness, each mass-loading scenario was tested three times. An example of the time histories recorded by the camera-based system and the laser distance meter is presented in Figure 2a, while Figure 2b displays the corresponding frequency domain response obtained using a Fast Fourier Transform (FFT). As shown, the two signals exhibit strong correlation, with peak-to-peak amplitudes of 26.81 ± 1 and 25.43 ± 2.02 for the camera and laser measurements, respectively. In the frequency domain, both signals reveal a distinct and consistent peak at 40 Hz, corresponding to the imposed rotational speed of 2,400 rpm, further confirming the agreement between the two sensing modalities.

Since each test was repeated three times, it was possible to compute the mean and standard deviation of the measured amplitudes from both systems, enabling a quantitative comparison of their performance. These results are summarized in Figure 3. As observed, the measurements obtained from the camera-based system using OMM closely match those from the laser sensor, with all data points falling within one standard deviation of difference. This consistency validates the accuracy and reliability of the camera-based method in replicating the reference measurements provided by the laser displacement sensor. Since the system developed in this study is ultimately intended for inspecting operational hydropower turbines, where close camera placement may not be feasible, a second laboratory experiment was conducted to evaluate the performance of OMM as a function of working distance, field of view (FOV), and the camera's noise floor. In this experiment, the noise floor

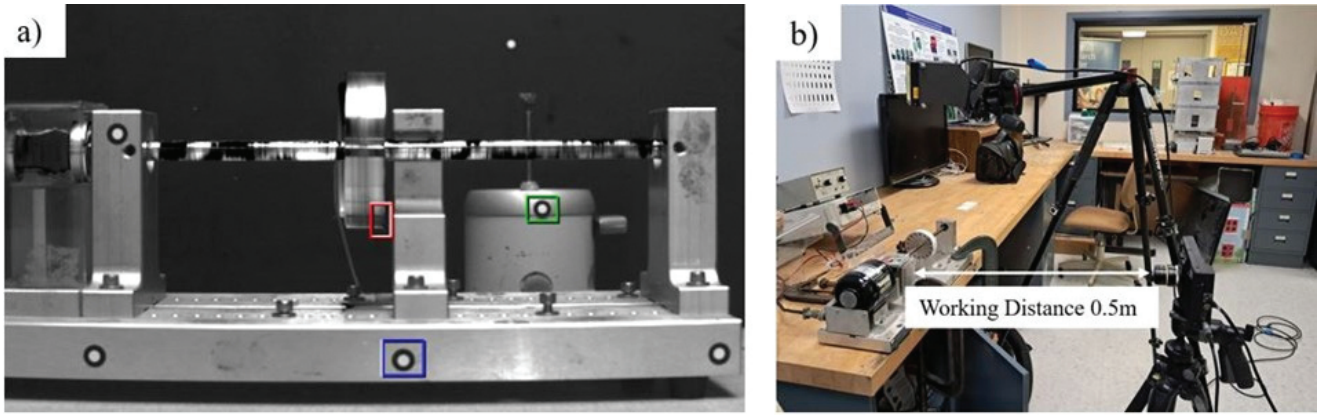


Fig. 1 Overview of the laboratory experiments used to validate the accuracy of OMM compared to traditional laser-based measurements: a) axle test rig as viewed by the IRIS MS camera and b) experimental setup.

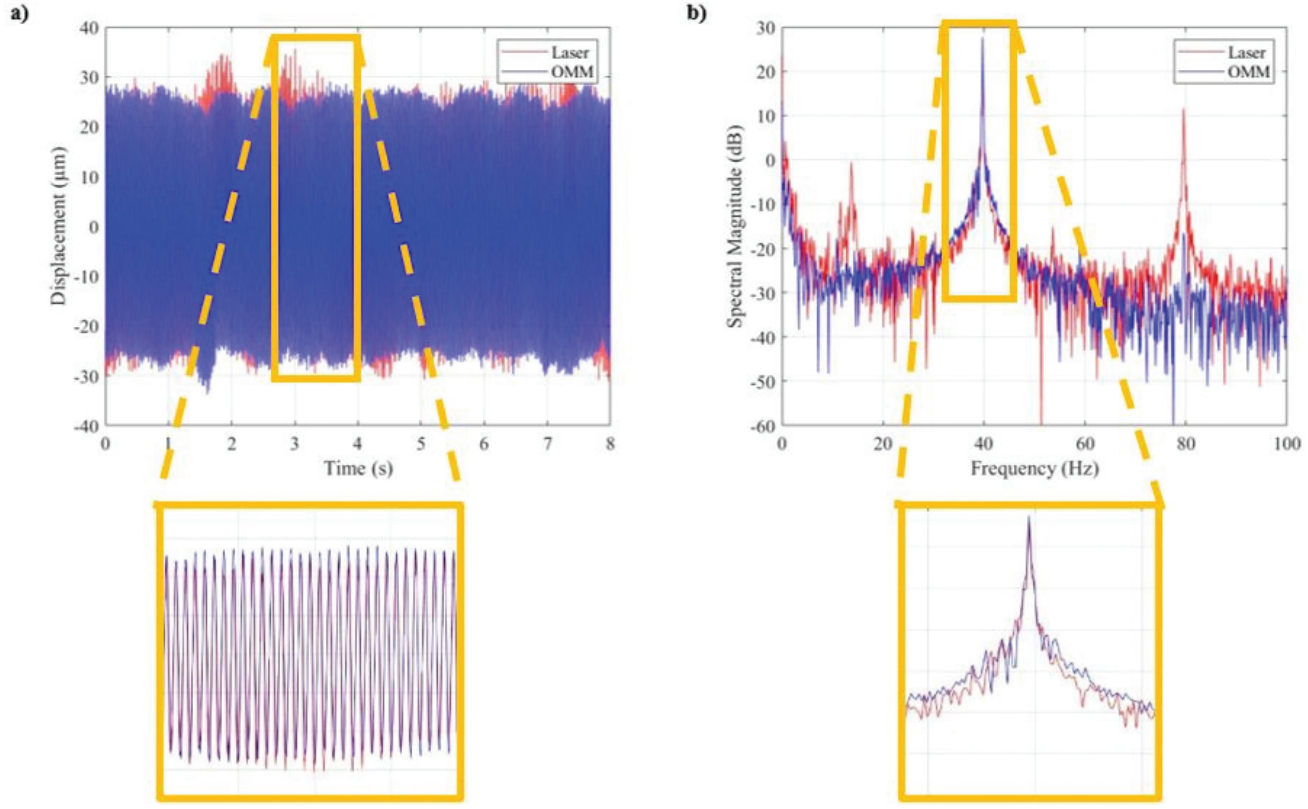


Fig. 2 Example of displacement signals in the Y-direction collected with the laser displacement sensor and the camera-based system for the case in which a mass of $6 \cdot 10^{-3}$ kg was added to the axle test rig: a) time domain results and b) corresponding frequency spectra.

of the camera was quantified by imaging a static, non-vibrating scene at working distances ranging from 1 to 7 meters, in 1-meter increments. The resulting measures, which provide insight into how signal quality degrades with increasing distance, are presented in Figure 4.

In this context, the noise floor is defined as the root mean square (RMS) of the signal measured along the x- and y-axes. Under ideal conditions, given that the camera images a stationary target, the measured displacement should be zero. However, due to inherent sensor noise, the camera produces displacement readings typically ranging between 5 and 40 μm. As expected, the noise floor of the camera-based system increases with working distance, which also corresponds to an increase in the field of view (FOV) and a reduction in spatial resolution.

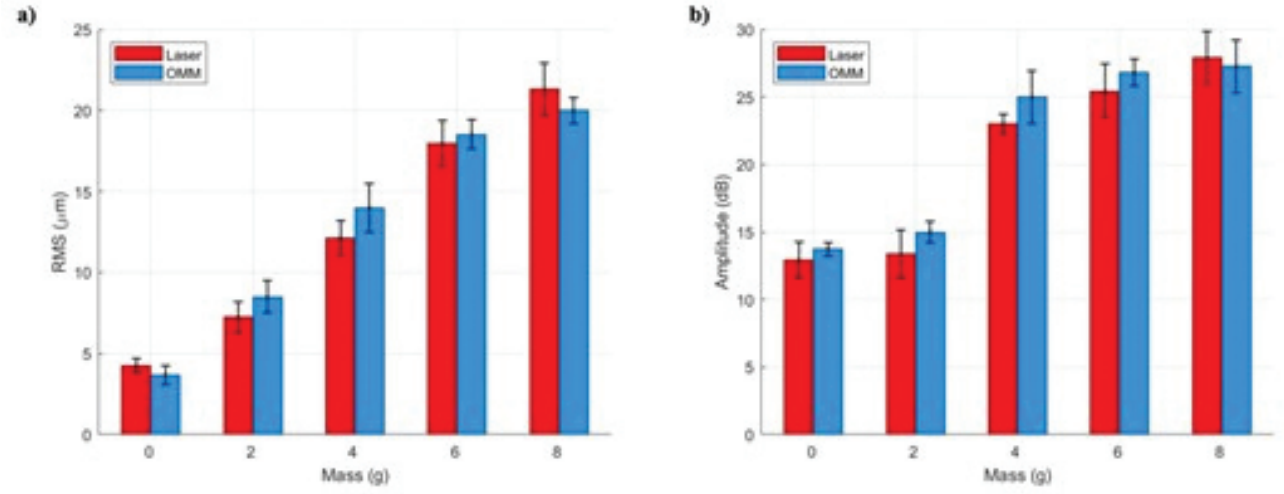


Fig. 3 Comparison of results obtained in the first laboratory experiment for all the case studies considered: a) time domain comparison and b) frequency domain comparison.

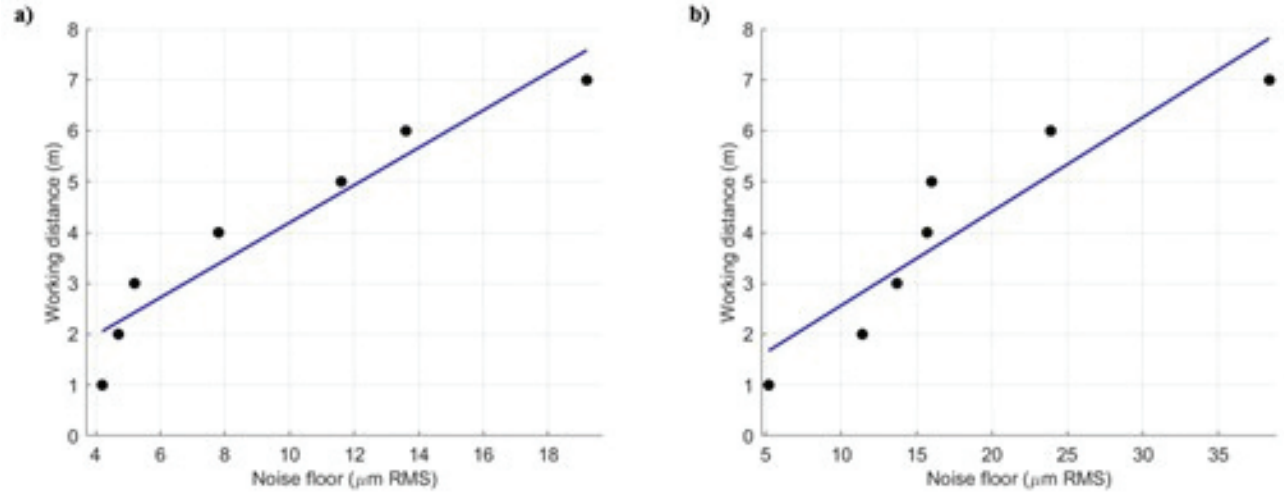


Fig. 4 IRIS MX's noise floor as a function of the working distance expressed in terms of the signal's RMS in the a) X-direction and b) Y-direction.

To assess the viability of the OMM system for measuring displacement at working distances beyond 1 meter, a third laboratory experiment was conducted. In this test, a target object was mounted on a shaker and excited with a 3 Hz sinusoidal input. The vertical displacement of the object was simultaneously measured using both the camera-based system and a laser displacement sensor. Measurements were collected at working distances ranging from 1 to 7 meters, in 1-meter increments. To ensure statistical robustness, each test condition was repeated three times. Representative results obtained at 1 m and 7 m working distances are illustrated in Figure 5.

As shown in Figure 5a, the time series at a working distance of 1 meter reveals strong agreement between the camera-based system and the laser displacement sensor, with nearly indistinguishable waveforms. This close match indicates that the camera-based system is capable of accurately replicating the reference measurements at short range. Figure 5b provides a quantitative comparison using the Time Response Assurance Criterion (TRAC), confirming a correlation above 99% between the two signals. At a working distance of 7 meters, the results in Figure 5c show a somewhat reduced level of agreement; nevertheless, the camera-based system still successfully captures the displacement of the target. In this case, Figure 5d shows a TRAC value of approximately 95%, with the scatter plot exhibiting greater dispersion around the unity line, indicating a modest decline in measurement accuracy. Despite this reduction, the results confirm that OMM remains a viable and reliable

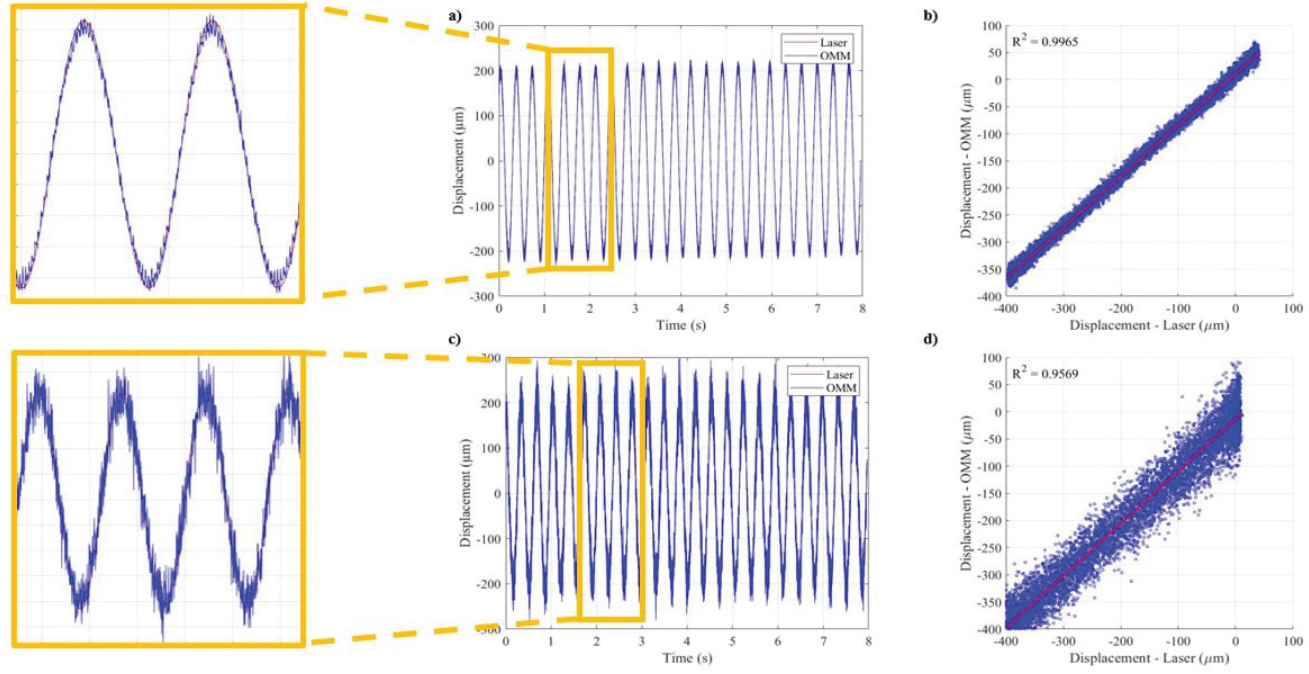


Fig. 5 Comparison of signals measured with the camera-based system at different working distances against laser distance sensors: a) time series at 1 m working distance, b) corresponding TRAC between the two datasets, c) time series at 7 m working distance, and d) corresponding TRAC between the two datasets.

technique for displacement measurement even at extended working distances, with only a minor degradation in performance compared to the reference sensor.

Field Tests

The field tests described in this paper were conducted at the Boott Hydropower Plant in Lowell, MA, on an 8.65 MW horizontal Francis turbine manufactured by Fuji Electric (see Figure 6a). The turbine operates with a head of ∼12 m and a rotational speed of 120 rpm (i.e., 2 Hz), creating a dynamic yet controlled environment for experimental validation. The goal of these tests was to validate OMM's accuracy and reliability in measuring the displacement of turbine components under real operating conditions and to compare its performance with that of conventional sensors, such as laser displacement sensors and proximity probes.

To collect the necessary data, three different sensing modalities were deployed: the 5-megapixel IRIS MX camera operating at 125 frames per second, the Keyence LK-G402 laser displacement sensor sampling at 1,000 Hz, and pre-installed proximity probes on the turbine shaft. As shown in Figure 6b and Figure 6c, the camera was positioned at two distinct working distances: 2.70 meters from Shaft 1 and 2.27 meters from Shaft 2. In both tests, the camera was used to measure the vertical displacement (i.e., Y-direction) of the two shafts as they vibrated during turbine operation. The proximity probes, installed on the turbine by the plant's management company, are used to record displacements along both the Y- and Z-directions for Shaft 1 and the Y-direction for Shaft 2. Similarly, the laser sensor mounted near Shaft 1 was used to measure the displacement of this component in the Z-direction (see Figure 6d). Each configuration was tested twice to ensure the reproducibility of results and enable statistical analysis.

The results of the tests are shown in Figure 7. In Figure 7a, the data obtained for Shaft 1 show that the average peak-to-peak displacement in the Y-direction measured using OMM was 162 ±8.5 μm. This value was corroborated by the reading of the proximity probe measurements, which showed close agreement, confirming the camera's capability to resolve motion at these distances with acceptable precision. These results were visualized using a series of images comparing different magnification levels (α = 0, 50, and 100), emphasizing how motion becomes more visually interpretable with increased magnification. As shown in Figure 7b, the OMM analysis produced an average peak-to-peak Y-displacement of 129±3.5 μm. This value was likewise validated against proximity probe data, with a minimal difference between the two methods.

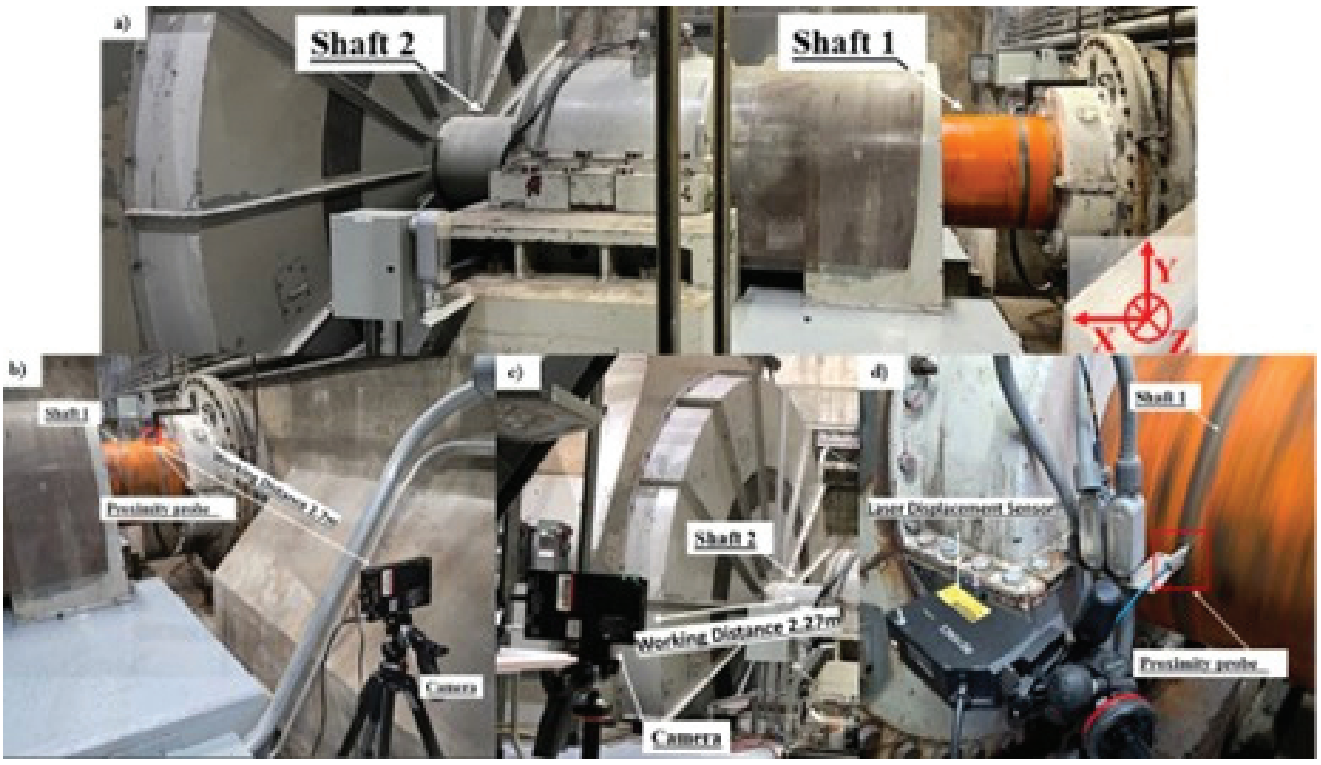


Fig. 6 8.65 MW horizontal Francis turbine at the Boott Hydropower Plant in Lowell, MA used to perform the field tests: a) overview of the turbine showing the two shafts inspected during the tests and indication of the X-Y-Z reference system used, b) experimental setup showing the camera and the proximity probe locations with reference to Shaft 1 used to measure displacements in the Y-direction, c) experimental setup showing the camera locations with reference to Shaft 2 used to measure displacements in the Y-direction, and d) view of the area behind Shaft 1 showing the location of the laser displacement sensor and the second proximity probe to measure displacements in the Z-direction.

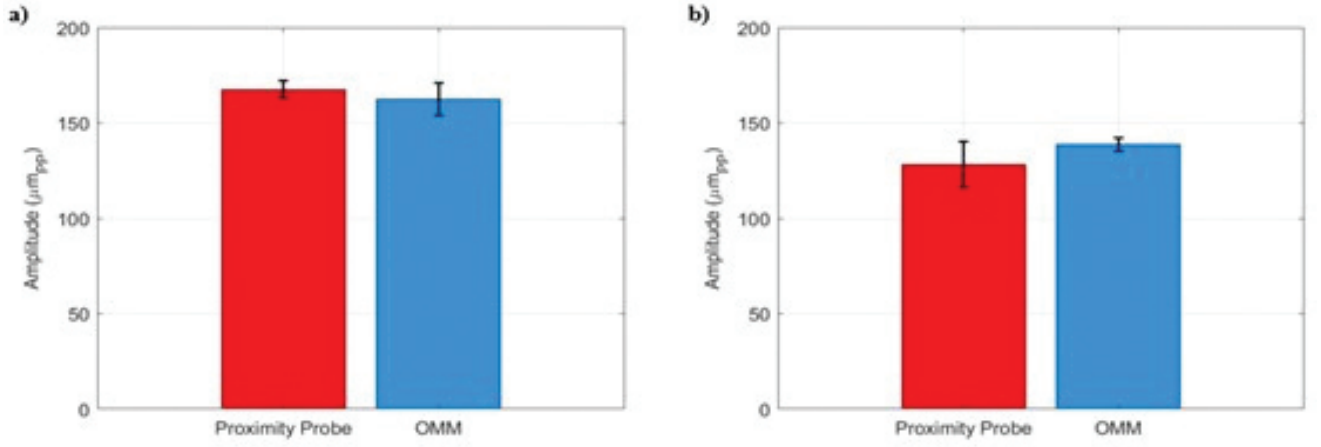


Fig. 7 Comparison of the results obtained with OMM and the proximity probes during the field tests: a) results for shaft 1 and b) results for shaft 2.

Conclusion

In summary, the field tests demonstrated that OMM is capable of capturing small-amplitude displacements on the order of 100 μm in a real hydropower environment, even when the camera is positioned at distances greater than 2 meters from the target. Error margins between OMM and traditional sensors ranged from 3% to 19%, with the overall performance of the

camera-based system deemed reliable for operational monitoring. These findings support the feasibility of deploying OMM for condition monitoring in hydropower applications, though further testing is recommended to refine its capabilities and ensure robustness across varying operational scenarios.

Acknowledgments This work relates to the Department of Navy award N00014-23-1-2124 issued by the Office of Naval Research (ONR). The U.S. Government has a royalty-free license throughout the world in all copyrightable material contained herein. The authors would like to thank the staff and personnel of the Boott Hydropower Plant for providing access to the facility used during the field campaign and assisting with testing.

References

1. Bandara, S., Rajeev, P., & Gad, E. (2024). A review on condition assessment technologies for power distribution network infrastructure. *Structure and Infrastructure Engineering*, *20*(11), 1834-1851.
2. Wang, J., Xu, C., Zhang, J., & Zhong, R. (2022). Big data analytics for intelligent manufacturing systems: A review. *Journal of Manufacturing Systems*, *62*, 738-752.
3. Gagliardi, V., Tosti, F., Bianchini Ciampoli, L., Battagliere, M. L., D'Amato, L., Alani, A. M., & Benedetto, A. (2023). Satellite remote sensing and non-destructive testing methods for transport infrastructure monitoring: Advances, challenges and perspectives. *Remote Sensing*, *15*(2), 418.
4. Zhang, L., Pang, M., Bahaj, A. S., Yang, Y., & Wang, C. (2021). Small hydropower development in China: Growing challenges and transition strategy. *Renewable and Sustainable Energy Reviews*, *137*, 110653.
5. Betti, A., Crisostomi, E., Paolinelli, G., Piazzi, A., Ruffini, F., & Tucci, M. (2021). Condition monitoring and predictive maintenance methodologies for hydropower plants equipment. *Renewable Energy*, *171*, 246-253.
6. Baron, P., Kočiško, M., Hlavatá, S., & Franas, E. (2022). Vibrodiagnostics as a predictive maintenance tool in the operation of turbo generators of a small hydropower plant. *Advances in mechanical engineering*, *14*(5), 16878132221101023.
7. Zhang, G., Yu, R., Dai, L., & Pan, J. (2019). Condition monitoring and fault diagnosis of hydropower station units. *Academic Journal of Engineering and Technology Science*, *2*(2), 89-95.
8. Wadhwa, N., Rubinstein, M., Durand, F., & Freeman, W. T. (2013). Phase-based video motion processing. *ACM Transactions on Graphics (ToG)*, *32*(4), 1-10.
9. Chen, J. G., Wadhwa, N., Cha, Y. J., Durand, F., Freeman, W. T., & Buyukozturk, O. (2015). Modal identification of simple structures with high-speed video using motion magnification. *Journal of Sound and Vibration*, *345*, 58-71.
10. Tiboni, M., Remino, C., Bussola, R., & Amici, C. (2022). A review on vibration-based condition monitoring of rotating machinery. *Applied Sciences*, *12*(3), 972.
11. Romanssini, M., de Aguirre, P. C. C., Compassi-Severo, L., & Girardi, A. G. (2023). A review on vibration monitoring techniques for predictive maintenance of rotating machinery. *Eng*, *4*(3), 1797-1817.
12. Goyal, D., Mongia, C., & Sehgal, S. (2021). Applications of digital signal processing in monitoring machining processes and rotary components: A review. *IEEE Sensors Journal*, *21*(7), 8780-8804.
13. Verellen, T., Verbelen, F., Stockman, K., & Steckel, J. (2021). Beamforming applied to ultrasound analysis in detection of bearing defects. *Sensors*, *21*(20), 6803
14. Dao, F., Zeng, Y., Zou, Y., Li, X., & Qian, J. (2021). Acoustic vibration approach for detecting faults in hydroelectric units: A review. *Energies*, *14*(23), 7840.
15. Kundu, P. (2024). Review of rotating machinery elements condition monitoring using acoustic emission signal. *Expert Systems with Applications*, *252*, 124169.
16. Wang, R., Zhan, X., Bai, H., Dong, E., Cheng, Z., & Jia, X. (2022). A review of fault diagnosis methods for rotating machinery using infrared thermography. *Micromachines*, *13*(10), 1644.
17. Mehta, A., Goyal, D., Choudhary, A., Pabla, B. S., & Belghith, S. (2021). Machine Learning-Based Fault Diagnosis of Self-Aligning Bearings for Rotating Machinery Using Infrared Thermography. *Mathematical Problems in Engineering*, *2021*(1), 9947300.
18. Karna, A., Chitrakar, S., Neopane, H. P., & Dahlhaug, O. G. (2025). A review of condition monitoring in Francis turbines for predictive maintenance. *Journal of Vibration and Control*, 10775463251315816.
19. de Santis, R. B., Gontijo, T. S., & Costa, M. A. (2022). Condition-based maintenance in hydroelectric plants: A systematic literature review. *Proceedings of the Institution of Mechanical Engineers, Part O: Journal of Risk and Reliability*, *236*(5), 631-646.
20. Niezrecki, C., Baqersad, J., & Sabato, A. (2019). Digital image correlation techniques for NDE and SHM. In *Handbook of advanced nondestructive evaluation* (pp. 1545-1590). Springer, Cham.
21. Sabato, A., Dabetwar, S., Kulkarni, N. N., & Fortino, G. (2023). Noncontact sensing techniques for AI-aided structural health monitoring: a systematic review. *IEEE Sensors Journal*, *23*(5), 4672-4684.
22. Civera, M., Zanotti Fragonara, L., & Surace, C. (2020). An experimental study of the feasibility of phase-based video magnification for damage detection and localisation in operational deflection shapes. *Strain*, *56*(1), e12336.
23. Le Ngo, A. C., Johnston, A., Phan, R. C. W., & See, J. (2018, May). Micro-expression motion magnification: Global lagrangian vs. local eulerian approaches. In *2018 13th IEEE international conference on automatic face & gesture recognition (FG 2018)* (pp. 650-656). IEEE.
24. Valente, N. A., do Cabo, C. T., Mao, Z., & Niezrecki, C. (2022). Quantification of phase-based magnified motion using image enhancement and optical flow techniques. *Measurement*, *189*, 110508.
25. Dragonetti, P., Civera, M., Miraglia, G., & Ceravolo, R. (2025). A Benchmark Dataset for the Validation of Phase-Based Motion Magnification-Based Experimental Modal Analysis. *Data (2306-5729)*, *10*(4).
26. Siringoringo, D. M., Wangchuk, S., & Fujino, Y. (2021). Noncontact operational modal analysis of light poles by vision-based motion-magnification method. *Engineering Structures*, *244*, 112728.

27. Rohe, D. P., & Reu, P. L. (2021). Experimental modal analysis using phase quantities from phase-based motion processing and motion magnification. *Experimental Techniques*, *45*(5), 297-312.
28. Luo, K., Kong, X., Li, J., Hu, J., & Deng, L. (2024). Motion magnification for video-based vibration measurement of civil structures: A review. *Mechanical Systems and Signal Processing*, *220*, 111681.
29. Čufar, K., Slavič, J., & Boltežar, M. (2024). Mode-shape magnification in high-speed camera measurements. *Mechanical Systems and Signal Processing*, *213*, 111336.
30. Civera, M., Zanotti Fragonara, L., Antonaci, P., Anglani, G., & Surace, C. (2021). An Experimental Validation of Phase-Based Motion Magnification for Structures with Developing Cracks and Time-Varying Configurations. *Shock and Vibration*, *2021*(1), 5518163.
31. Cosco, F., Cuenca, J., Desmet, W., Janssens, K., & Mundo, D. (2022). Towards phase-based defect detection: A feasibility study in vibrating panels. *Journal of Sound and Vibration*, *537*, 117196.
32. Nieduzak, T., Valente, N. A., Niezrecki, C., & Sabato, A. (2023, June). Optical Motion Magnification: A Comparative Study and Application for Vibration Analysis. In *Society for Experimental Mechanics Annual Conference and Exposition* (pp. 1-7). Cham: Springer Nature Switzerland.
33. Nieduzak, T. B., Kulkarni, N. N., Niezrecki, C., & Sabato, A. (2023). Wind Turbine Monitoring Using Optical Motion Magnification: Challenges and Opportunities. *STRUCTURAL HEALTH MONITORING 2023*.